

2022-05-20

# Microplastics captured by snowfall: A study in Northern Iran

Abbasi, S

<http://hdl.handle.net/10026.1/19185>

---

10.1016/j.scitotenv.2022.153451

Science of the Total Environment

Elsevier

---

*All content in PEARL is protected by copyright law. Author manuscripts are made available in accordance with publisher policies. Please cite only the published version using the details provided on the item record or document. In the absence of an open licence (e.g. Creative Commons), permissions for further reuse of content should be sought from the publisher or author.*

# 1           **Microplastics captured by snowfall: A study in Northern Iran**

2  
3   Sajjad Abbasi <sup>a,b</sup> \*, Mustafa Alirezazadeh <sup>a</sup>, Nastaran Razeghi<sup>c</sup>, Mahrooz Rezaei <sup>d</sup>, Haniye  
4   Pourmahmood <sup>e</sup>, Reza Dehbandi <sup>f</sup>, Meisam Rastegari Mehr <sup>g</sup>, Shirin Yavar Ashayeri <sup>a</sup>, Patryk  
5   Oleszczuk <sup>b</sup>, Andrew Turner <sup>h</sup>

6  
7   <sup>a</sup> Department of Earth Sciences, College of Science, Shiraz University, Shiraz 71454, Iran

8   <sup>b</sup> Department of Radiochemistry and Environmental Chemistry, Faculty of Chemistry, Maria  
9   Curie-Skłodowska University, Lublin 20-031, Poland

10   <sup>c</sup> Department of Environment Science and Engineering, Faculty of Natural Resources, University  
11   of Tehran, P.O. Box 4314, Karaj 31587-77878, Iran

12   <sup>d</sup> Meteorology and Air Quality Group, Wageningen University & Research, PO. Box 47, 6700  
13   AA Wageningen, the Netherlands.

14   <sup>e</sup> Department of Soil Science, School of Agriculture, Shiraz University, Shiraz, Iran

15   <sup>f</sup> Environmental Technologies Research Center, Ahvaz Jundishapur University of Medical  
16   Sciences, Ahvaz, Iran

17   <sup>g</sup> Department of Applied Geology, Faculty of Earth Sciences, Kharazmi University, Tehran, Iran

18   <sup>h</sup> School of Geography, Earth and Environmental Sciences, University of Plymouth, Plymouth  
19   PL4 8AA, UK

20  
21   Corresponding Author: Sajjad Abbasi; Department of Earth Sciences, College of Science, Shiraz  
22   University, Shiraz 71454, Iran & Department of Radiochemistry and Environmental Chemistry,  
23   Faculty of Chemistry, Maria Curie-Skłodowska University, Lublin 20-031, Poland

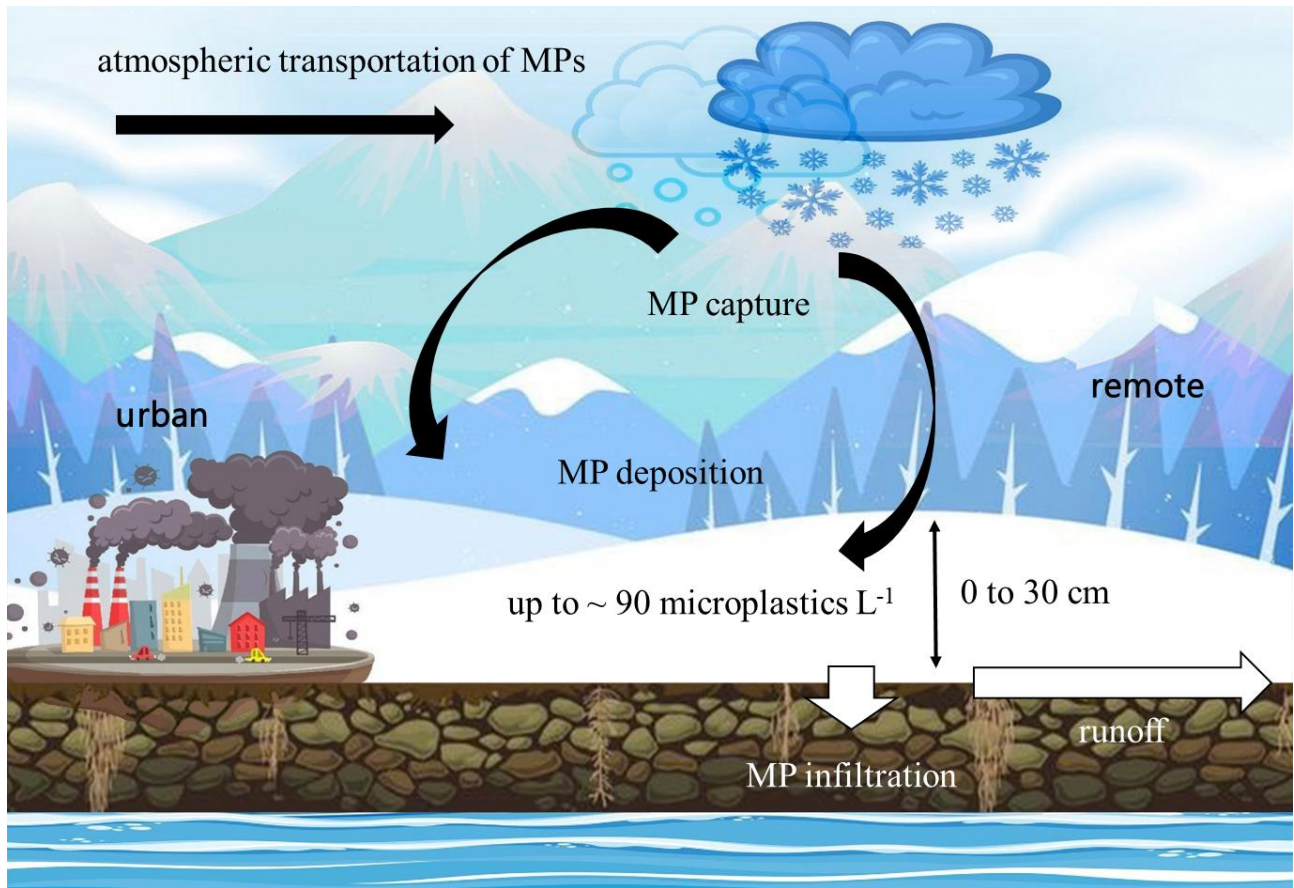
24   E-mail Address: [sajjad.abbasi.h@gmail.com](mailto:sajjad.abbasi.h@gmail.com); [sajjad.abbasi@shirazu.ac.ir](mailto:sajjad.abbasi@shirazu.ac.ir);  
25   [sajjad.abbasi@mail.umcs.pl](mailto:sajjad.abbasi@mail.umcs.pl)

26   Accepted 22 January 2022

27   <http://dx.doi.org/10.1016/j.scitotenv.2022.153451>



33 **Graphical Abstract**



34

35

36 **Highlights**

37 Microplastics (MPs) have been observed in fresh snow in northern Iran

38 MPs were heterogeneously distributed throughout the region and at different depths

39 Mean and median concentrations were  $\sim 20$  and  $12 \text{ MP L}^{-1}$ , respectively

40 Snow appears to capture a greater diversity of MP sizes and shapes than rainfall

41 The significance of snow to the global transport of MPs requires further study.

42

43

44

45 **Abstract**

46 Samples of fresh snow ( $n = 34$ ) have been collected from 29 locations in various urban and remote  
47 regions of northern Iran following a period of sustained snowfall and the thawed contents  
48 examined for microplastics (MPs) according to established techniques. MP concentrations ranged  
49 from undetected to 86 MP L<sup>-1</sup> (mean and median concentrations ~ 20 MP and 12 MP L<sup>-1</sup>,  
50 respectively) and there was no significant difference in MP concentration between sample location  
51 type or between different depths of snow (or time of deposition) sampled at selected sites. Fibres  
52 were the dominant shape of MP and  $\mu$ -Raman spectroscopy of selected samples revealed a variety  
53 of polymer types, with nylon most abundant. Scanning electron microscopy coupled with energy-  
54 dispersive X-ray analysis showed that some MPs were smooth and unweathered while others were  
55 more irregular and exhibited significant photo-oxidative and mechanical weathering as well as  
56 contamination by extraneous geogenic particles. These characteristics reflect the importance of  
57 both local and distal sources to the heterogeneous pool of MPs in precipitated snow. The mean and  
58 median concentrations of MPs in the snow samples were not dissimilar to the published mean and  
59 median concentrations for MPs in rainfall collected from an elevated location in southwest Iran.  
60 However, compared with rainfall, MPs in snow appear to be larger and more diverse in their shape  
61 and composition (and include rubber particulates), possibly because of the greater size but lower  
62 terminal velocities of snowflakes relative to raindrops. Snowfall represents a significant means by  
63 which MPs are scavenged from the atmosphere and transferred to soil and surface waters that  
64 warrants greater attention.

65 **Keywords:** snow; precipitation; atmosphere; deposition; scavenging; fibres; flux

66

67

68

69

## 70 **1. Introduction**

71 It is becoming increasingly evident that the atmosphere is a highly important reservoir and  
72 transporter of microplastics (MPs). Sources to the atmosphere include emissions from industry,  
73 urban-suburban centres and agriculture during all stages of the plastic life cycle (Zhang et al.,  
74 2020). Airborne MPs are eventually deposited in the terrestrial and marine environments through  
75 dry or wet deposition, although many MPs, and in particular those with favourable aerodynamic  
76 properties like fibres, may be transported long distances (100s to 1000s of km) with regional air  
77 masses before this takes place (Brahney et al., 2020; Allen et al., 2021). Consequently, MPs are a  
78 global problem, with plastic reported in a diversity of regions remote from any significant sources,  
79 including the Arctic (Bergmann et al., 2019), the central Pacific Ocean (Liu et al., 2020) and the  
80 Himalayas (Napper et al., 2020). Once deposited, MPs may be captured by soil, lost to ground  
81 water or entrained by surface water bodies, or may be resuspended by wind or through bubble  
82 burst ejection in breaking waves (Allen et al., 2020).

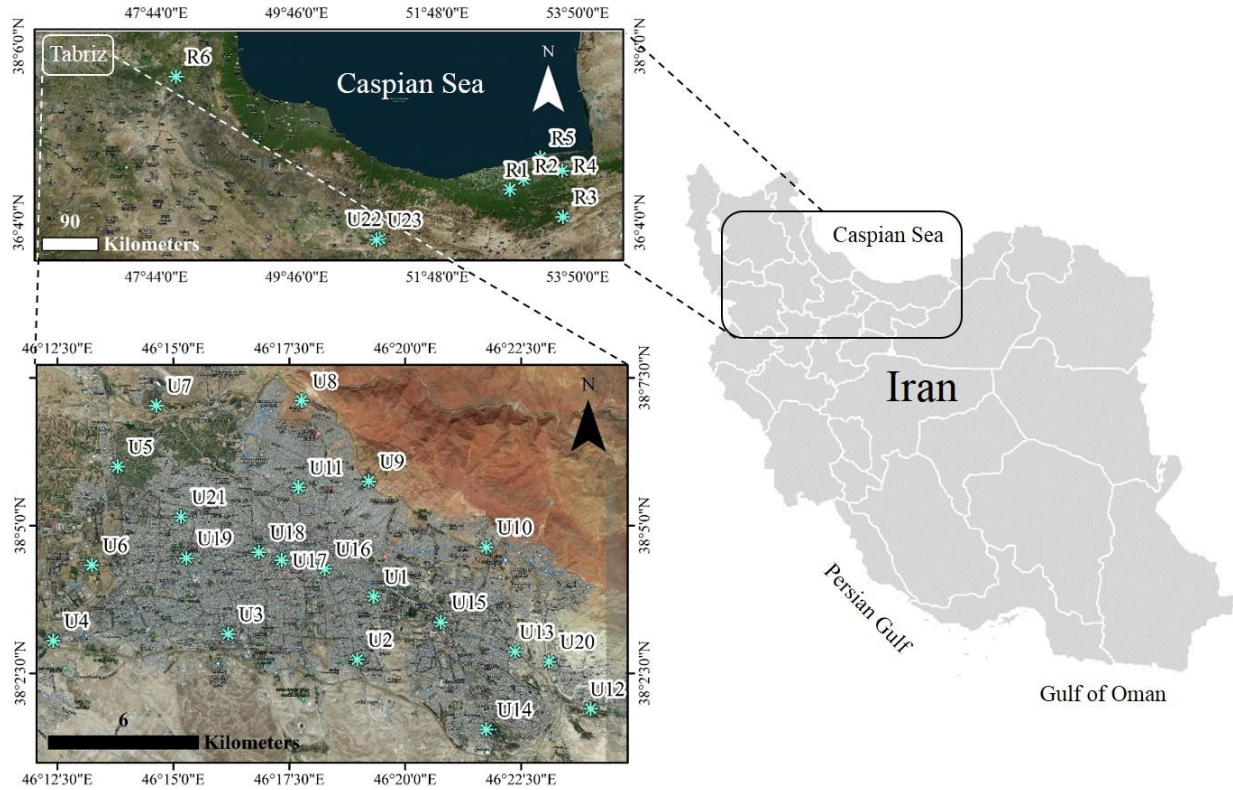
83 Atmospheric MPs are usually collected passively with a sampling device that provides a location  
84 and time specific indication of MP fluxes associated with rainfall and/or dry deposition (Dris et  
85 al., 2017; Klein and Fisher, 2017; Abbasi and Turner, 2021). However, despite its importance to  
86 global precipitation and the water cycle (Skofronick-Jackson et al., 2019) and evidence for an  
87 increase in frequency with climate change (Zhu et al., 2012), relatively little information exists on  
88 the mechanisms and significance of snowfall in capturing and depositing MPs. Moreover, most  
89 studies consider MP accumulation in Arctic or alpine environments (Bergmann et al., 2019;

90 Huntington et al, 2020; Parolini et al., 2021) where snow cover is permanent or occurs for long  
91 periods of the year and where MP capture (or scavenging) by falling snow and MP deposition on  
92 fallen snow may be difficult to distinguish. Snowflakes are larger, less dense and have lower  
93 terminal velocities than raindrops and one might expect them to capture and deposit different  
94 quantities and types of MPs. The gradual but continuous accumulation of snow during a single but  
95 protracted event also allows short-term temporal distributions of MP deposition and airborne MP  
96 contamination to be examined through different depths of snow accumulations.

97 In the present study, we describe, for the first time, the regional sampling of MPs in deposited  
98 snow arising from a single, sustained snowfall event. Samples were collected opportunistically  
99 from both urban and remote settings throughout northern Iran, and in some deposits snow was  
100 sampled at different depths. MPs were identified, quantified and characterised in melted samples  
101 using established techniques in order to better understand the role of this type of precipitation in  
102 scavenging and depositing MPs from the atmosphere.

103

104



105

106 **Figure 1: Map of the region under study. Locations pre-fixed with R and U are remote and**  
 107 **urban, respectively.**

108

109 **2. Materials and Methods**

110 *2.1 Study region and sampling*

111 Northern Iran encompasses various climatic types (including semiarid, cold semiarid and  
 112 Mediterranean) but snowfall is a common occurrence in the region under study (shown in Figure  
 113 1) during winter and when influenced by maritime polar air masses from the northwest and  
 114 continental polar air masses from Siberia to the north.

115 Twenty one “urban” locations (U1 to U21), including industrial zones, residential areas,  
 116 transportation hubs and green spaces, were sampled in Tabriz, a city to the west of the region with  
 117 a population of about 1.6 million and a mean elevation of about 1350 m above sea level. Tabriz is

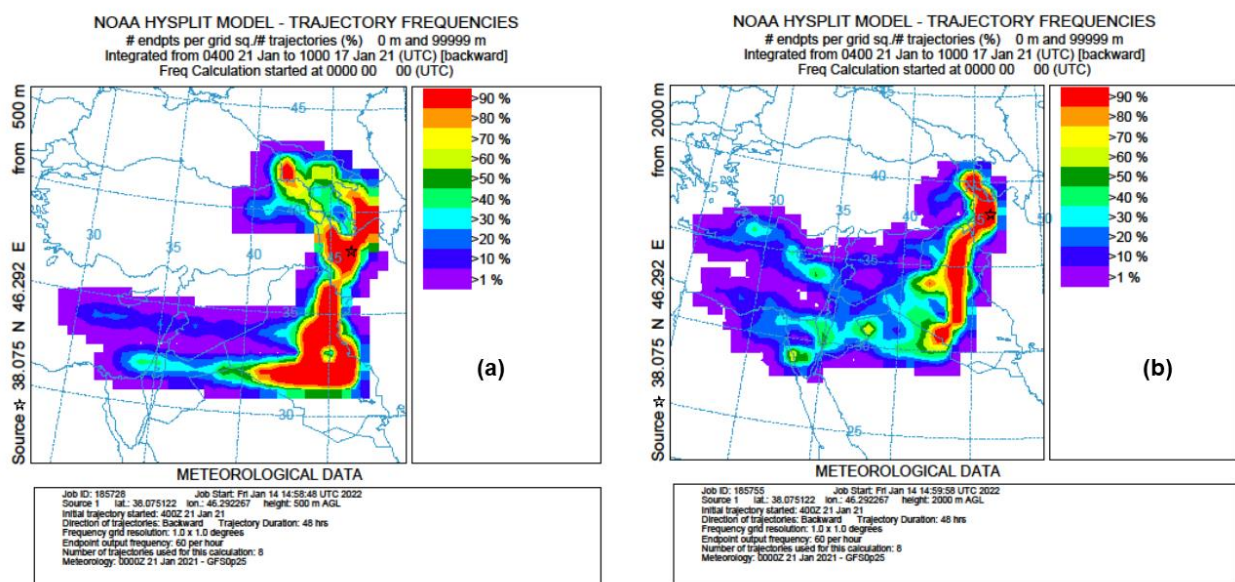


118 home to various manufacturing industries, including food, chemicals, electronic equipment and  
119 textiles, which contribute to anthropogenic pollutant emissions. Surrounded by mountains and  
120 subject to thermal inversions, the city often experiences poor urban air quality (Parsa et al., 2019).  
121 Two urban-industrial locations (U22 and U23) were also sampled in the hilly, northern reaches of  
122 the Tehran metropolis (population ~ 15 million) to the south east of Tabriz. Six locations were  
123 sampled from various, more “remote” areas to the south and south east of Tabriz (R1 to R6). These  
124 included small towns and villages within forested areas or on mountain slopes, and a remote  
125 location close to a thermal power station (R5).

126 Fresh, deposited snow samples were collected on 21<sup>st</sup> January, 2021, after a 12- to 15-hour period  
127 of sustained precipitation caused by the convergence of polar air from the north and milder air  
128 from the southwest. At each location, accessed by vehicle and/or on foot, and from the street, land  
129 surface or rooftops, snow was scraped into a 2-L glass jar that had been triple rinsed with filtered,  
130 distilled water (see below) using a stainless steel spoon by operators wearing cotton clothing and  
131 facing upwind. The depth of snow sampled, determined using a metal ruler, was 5 cm or 10 cm,  
132 but at four remote locations (R3, R4, R6) and one urban location (U23) where fresh deposits were  
133 sufficiently deep, snow was scraped from the surface (0 to 5 cm) and subsurface (5 to 15 cm) and,  
134 in one case (R6), from 15 to 30 cm. Sample jars (34 in total) were wrapped in aluminium foil to  
135 avoid external contamination before being transported to the laboratory, thawed, and stored under  
136 refrigeration at 4°C pending MP isolation.

137 On the same day and after the precipitation event, a 25-cm diameter, pre-washed metallic pot  
138 containing 500 mL of filtered, distilled water, was deployed for 12 h on the rooftop of a domestic  
139 property near to site U1 in the city of Tabriz in order to evaluate the significance of dry deposition.  
140 The sample was subsequently wrapped in aluminium foil and stored as above.

141 The potential source range of MPs associated with the period of snowfall was evaluated from 48-  
 142 h back trajectories from 17<sup>th</sup>/18<sup>th</sup> to 21<sup>st</sup> January, calculated using the National Oceanic and  
 143 Atmospheric Administration online software, Hybrid Single Particle Lagrangian Integrated  
 144 Trajectory (HYSPLIT) v4, and Global Forecast System (0.25 degree global) meteorological data.  
 145 Backward trajectories of 48 h in duration were calculated at six-hour intervals and at a resolution  
 146 of 1 degree, and at heights of 500 m and 2000m above ground level (and above the gradient height  
 147 for open terrain and large cities). Trajectories were integrated as frequency distributions which are  
 148 illustrated in Figure 2. Consistent with the meteorological conditions during and immediately  
 149 before sampling, air was brought into the region principally from southwesterly and northerly  
 150 directions, with a greater northwesterly component at the lower height of 500 m. The range of  
 151 influence, defined by the distance of the 1% trajectory frequency from Tabriz, extends to about  
 152 750 km to the northwest and 2500 km to the southwest at a height of 500 m, and to about 300 km  
 153 to the north and 3000 km to the southwest at a height of 2000 m.



154

155 **Figure 2: Trajectory frequencies calculated for Tabriz (starred) in northern Iran using**  
156 **HYSPLIT over a 48-h period and at six-hourly intervals for heights of (a) 500 m and (b) 2000**  
157 **m.**

158

## 159 *2.2 Isolation of microplastics*

160 To minimise contamination, all glass-ware and metal-ware used for sample processing,  
161 manipulation and analysis had been washed three times with filtered (S&S blue band, 2  $\mu\text{m}$ ),  
162 distilled water and stored in aluminium foil, and all sample processing was undertaken in a  
163 customized clean laboratory.

164

165 Thawed snow samples and the water capturing dry deposition were removed from refrigeration  
166 and allowed to reach room temperature. Using a graduated cylinder, 500 mL of each sample was  
167 transferred to a series of 1-L beakers. An appropriate quantity of filtered ( $< 2 \mu\text{m}$ )  $\text{ZnCl}_2$  (Arman  
168 Sina, Tehran) was added to each beaker and the contents agitated with glass-covered magnetic  
169 stirrers to attain saturated solutions of density  $\sim 1.8 \text{ g cm}^{-3}$ . Each solution, plus beaker rinses of  $\sim$   
170 20 mL saturated  $\text{ZnCl}_2$ , was then transferred to a series of 600 mL separation funnels and the  
171 contents were allowed to settle overnight. The upper 100 mL of each solution was retained in the  
172 funnels after discarding the remaining contents before aliquots of 100 mL of 30% filtered ( $< 2 \mu\text{m}$ )  
173  $\text{H}_2\text{O}_2$  (Arman Sina, Tehran) were added for 12 h to destroy organic matter. The contents of each  
174 funnel, plus triple 20-mL rinses of filtered, distilled water, were filtered through 1  $\mu\text{m}$  Johnson  
175 cellulose test membranes to capture MPs, with filters subsequently dried in glass petri dishes and  
176 under desiccation for 48 h. Procedural blanks, processed likewise but using 500 mL of filtered ( $<$   
177 2  $\mu\text{m}$ ), distilled water in place of snow melt samples, revealed no contamination from exposure to  
178 laboratory conditions.

179

### 180 *2.3 Identification and characterisation of microplastics*

181 MPs retained on each filter were visually identified, counted and characterised under a binocular  
182 microscope (Carl-Zeiss, Köln, Germany) at up to 200-x magnification using a 250 µm-diameter  
183 stainless steel probe and ImageJ software. MP identification, and with a size detection limit of  
184 about 30 to 50 µm, was based on shininess, thickness, hardness, surface and cross sectional  
185 structures, and reaction (melting or curling) in the presence of the heated probe (Abbasi et al.,  
186 2019). Classification was based on shape (fibre, film, fragment or spherule), length of the longest  
187 axis,  $L$  ( $L \leq 100 \mu\text{m}$ ,  $100 < L \leq 250 \mu\text{m}$ ,  $250 \leq L < 500 \mu\text{m}$ ,  $500 \leq L < 1000 \mu\text{m}$ ,  $L > 1000 \mu\text{m}$ )  
188 and colour (black-grey, yellow-orange, white-transparent, red-pink or blue-green).

189 The polymeric construction of 47 MPs of a range of shapes, sizes and colours and collected from  
190 different locations was determined using a micro-Raman spectrometer ( $\mu$ -Raman-532-Ci,  
191 Avantes, Apeldoorn, Netherland) with a laser of 785 nm and Raman shift of 400-1800  $\text{cm}^{-1}$ . Under  
192 the microscope and with the aid of a needle and tweezers, MPs were transferred to conductive  
193 copper adhesive and polymers were identified by comparing spectra with online, open access data  
194 on hosted at Open Specy (<https://wincowger.shinyapps.io/OpenSpecy/>) (Cowger et al., 2021).  
195 These MPs were subsequently mounted on microscope slides and gold-coated before being  
196 analysed under a high vacuum scanning electron microscope (SEM; TESCAN Vega 3, Czech  
197 Republic) equipped with an energy-dispersive X-ray microanalyser (EDX) and operated at a  
198 distance of about 15 mm and with a resolution of 2 nm and an accelerating voltage of 20 kV.

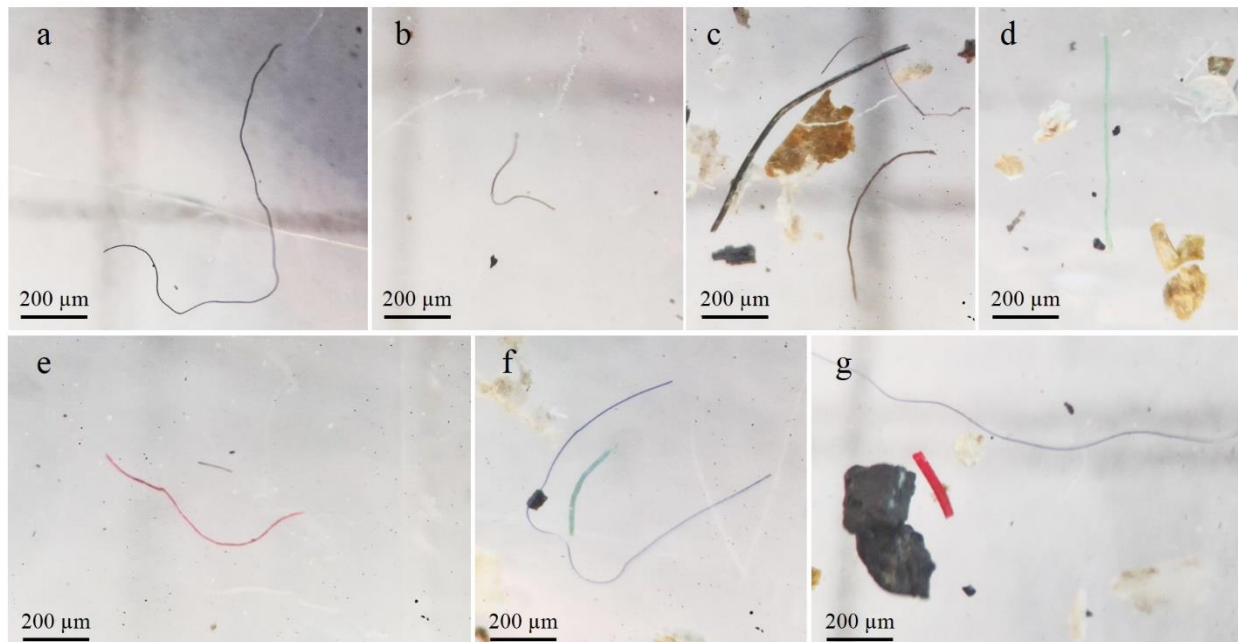
199

## 200 **3. Results**

201 In total, 348 particles were identified microscopically as MPs amongst the 34 snow samples  
202 considered, with a selection illustrated in Figure 3. MP abundance in individual samples ranged  
203 from zero at site U8, the most sheltered (by mountains) and most northerly location in Tabriz, to  
204 over 40 at sites U12 and U18, located in the central and eastern reaches of the city, respectively.  
205 The mean and median numbers of MPs in the urban and remote samples were 11.3 and 6.0, and  
206 8.7 and 4.0, respectively, and quantities were not significantly different between sample location  
207 type ( $p = 0.299$ ) according to a Mann-Whitney test. Where samples were taken from the surface  
208 (0 to 5 cm) and subsurface (5 to 15 cm) ( $n = 4$ ), the mean and median numbers of MPs were 9.3  
209 and 10, and 6.5 and 5.0, respectively, and no significant difference ( $p > 0.440$ ) was returned from  
210 a Kruskal-Wallis test.

211 A summary of the MPs by shape and colour is given in Table 1. Fibres comprised 90% of MPs  
212 and were represented by all colour categories but with black-grey the most abundant. Films and  
213 fragments contributed about 2% each to the total MP pool but while white-transparent and blue-  
214 green films and/or fragments were only detected in rural samples, most black-grey films and  
215 fragments were encountered in the urban setting. Significantly, all 16 spherules identified were  
216 black and originated from the rural sample in the vicinity of a thermal power station (R5).

217



218  
 219 **Figure 3: A selection of fibrous MPs in various snow samples identified under the**  
 220 **microscope. Note the presence of biological debris in (c) and (d) and a black rubber particle**  
 221 **in (g).**

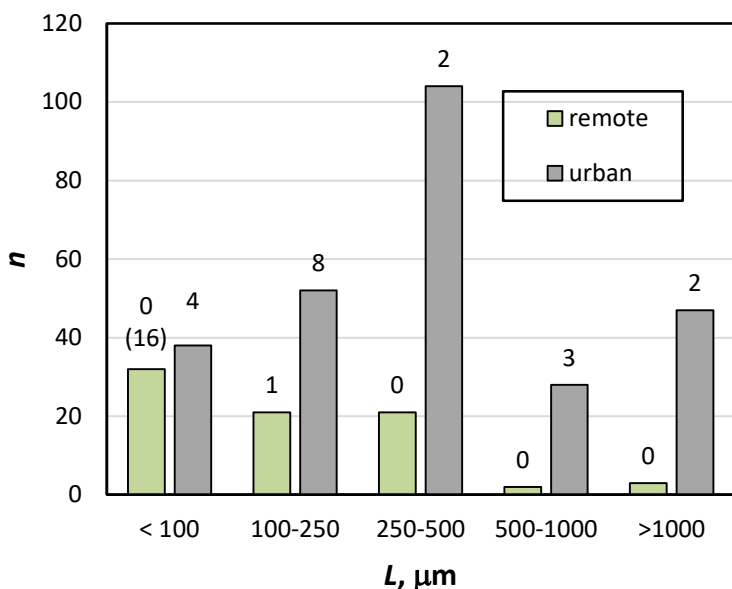
222  
 223 **Table 1: Distribution of the MPs identified in the snow samples, including those below the**  
 224 **surface, according to shape and colour.**

	white-transp.	yellow-orange	red-pink	black-grey	blue-green
fibres ( $n = 312$ )	36	11	50	128	87
films ( $n = 11$ )	1	0	0	10	0
fragments ( $n = 9$ )	6	0	0	2	1
spherules ( $n = 16$ )	0	0	0	16	0
total ( $n = 348$ )	43	11	50	156	88

225  
 226  
 227 Figure 4 shows the size distribution of the MPs in the urban and remote snow samples, along with  
 228 the frequency of non-fibrous particles in each category. The highest numbers of MPs occur in the  
 229 250 to 500  $\mu\text{m}$  fraction for urban snow and the  $< 100 \mu\text{m}$  fraction for remote snow. Only one film-  
 230 fragment was observed in the remote snow samples (or 1.2% of total MPs), while the frequency

231 of the 20 films and fragments in urban snows (or 7.4% of total MPs) is weighted towards the finer  
 232 particle fractions. Note that the spherical particles referred to above were all below 100  $\mu\text{m}$  in  
 233 length.

234



235

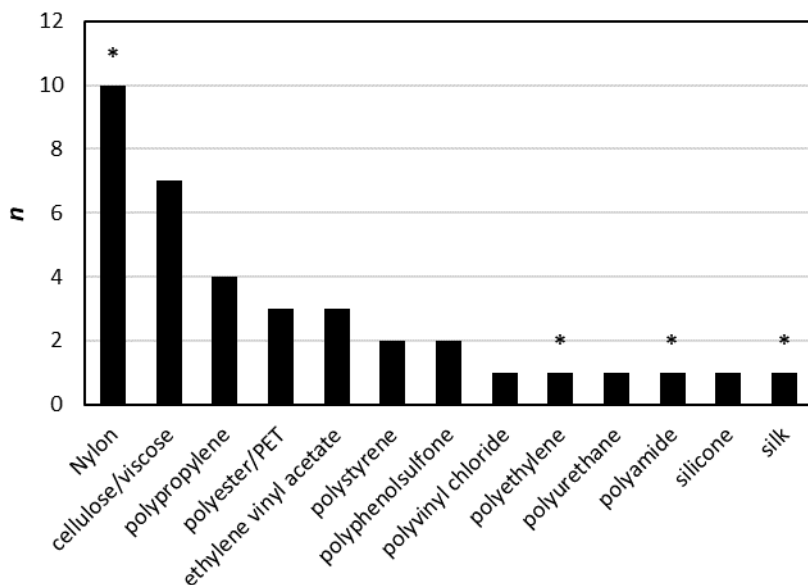
236 **Figure 4: Distribution of MPs by size in the urban and remote snow samples, including**  
 237 **those below the surface. Numbers above the bars correspond to the number of films and**  
 238 **fragments in each category, and the single number in parentheses refers to the number of**  
 239 **spherules observed at a single location.**

240

241 Figure 5 illustrates the distribution of MPs according to polymer type identified by Raman  
 242 spectroscopy. Here, and of the 47 samples analysed, 10 could not be matched with reference  
 243 libraries and 13 polymer types were identified. Most samples were petroleum-based  
 244 thermoplastics, but one was an elastomer (silicone), one was a natural polymer (silk) and seven

245 were cellulose-based. Since plant material is generally destroyed by H<sub>2</sub>O<sub>2</sub> (Prato et al., 2019), we  
246 infer that the cellulose polymers were synthetic in origin.

247



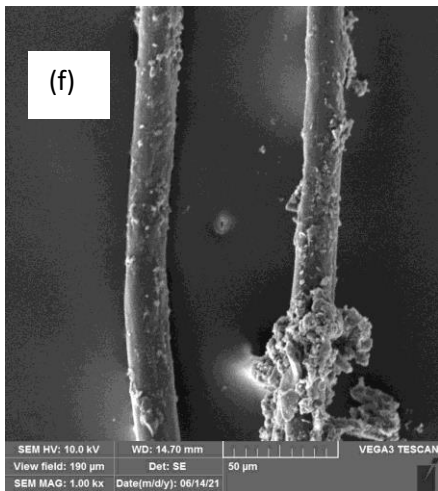
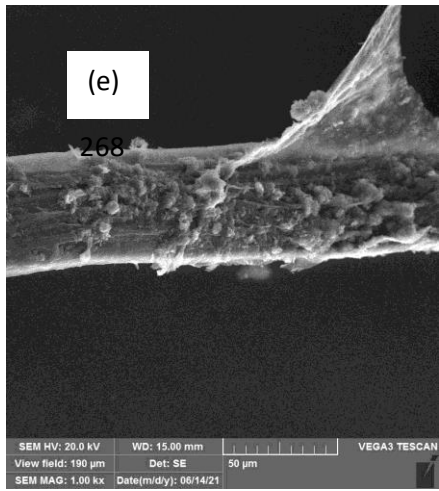
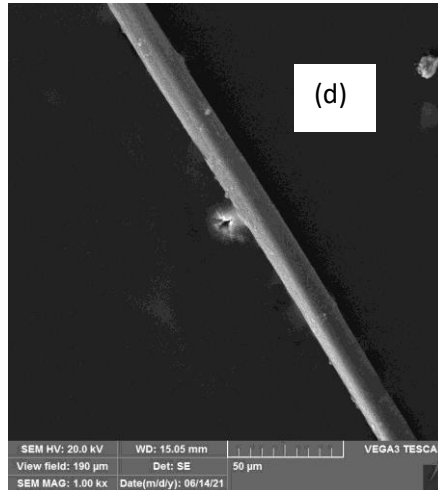
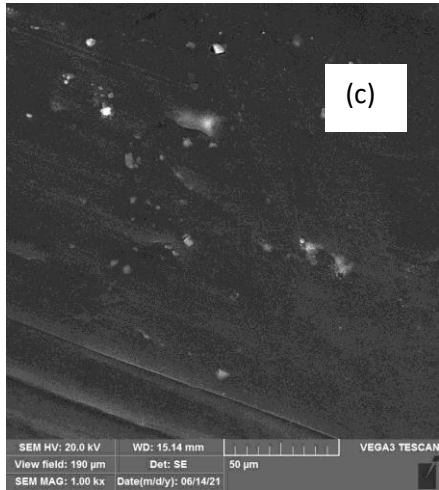
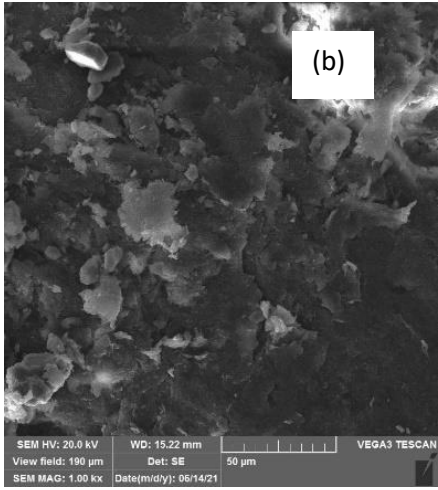
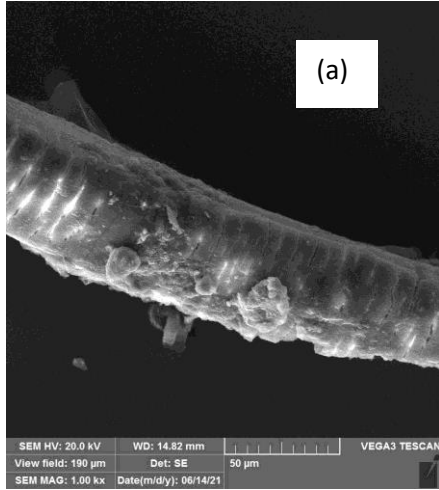
248

249 **Figure 5: Distribution of MPs ( $n = 37$ ) by polymer type. Asterisks denote that non-fibrous**  
250 **MPs (films and/or fragments) were amongst that category.**

251



252  
253  
254  
255  
256  
257  
258  
  
259  
260  
261  
262  
263  
264  
265  
  
266  
267  
268  
269  
270  
271  
272  
273  
274



275 **Figure 6: SEM images of selected MPs from the snow samples. (a) A blue,**  
276 **polyphenolsulfone fibre, (b) a white, polyethylene film, (c) a white Nylon film, (d) a red,**  
277 **polypropylene fibre, (e) a red, cellulose-based fibre, (f) a transparent, Nylon fibre.**

278  
279 SEM images of fibrous and non-fibrous MPs are exemplified in Figure 6. Some samples exhibit  
280 smooth surfaces (e.g. Figures 6c and 6d), with EDX detecting only C and O. Other samples,  
281 however, exhibit different degrees of weathering and photo-oxidation (flaking, cracking and  
282 fracturing) both at the surface and below the surface. Contamination is also visible, with EDAX  
283 revealing particulates composed of combinations of two or more of Al, Ca, Mg, Si and Ti. The  
284 scale bars on these and other images indicate that the diameters of fibres ranged from about 5 to  
285 50  $\mu\text{m}$ .

286 In contrast, the distilled water capturing dry deposition for a 12-h period following the precipitation  
287 event returned just one MP. This was a black fibre between 100 and 250  $\mu\text{m}$  in length but that was  
288 not characterised by Raman spectroscopy or SEM.

289

#### 290 **4. Discussion**

291 Despite the atmospheric transportation of MPs receiving considerable attention over the past few  
292 years (Dris et al., 2017; Allen et al., 2019; Klein and Fischer, 2019; Brahney et al., 2020;  
293 Evangeliou et al., 2020; Roblin et al., 2020; González-Pleiter et al., 2021; Huang et al., 2021;  
294 Wang et al., 2021), there is very little published information on the role of snow in capturing,  
295 depositing and preserving airborne MPs (Bergmann et al., 2019; Huntington et al., 2020; Parolini  
296 et al., 2021). The present study is the first to compare MPs in freshly fallen snow from the same

297 meteorological event in urban and remote areas, and the first to examine MP distributions with  
298 depth in snow deposits.

299 For continuous deposition, a constant wind speed and direction and no post-depositional MP  
300 migration in snow, it would be reasonable to expect an increase in MP abundance with snow depth  
301 as MPs are increasingly washed (or “snowed”) out of the atmosphere over the period of  
302 precipitation. That our results only conform to this distribution in one case suggests that  
303 meteorological conditions and snow intensity may have been variable over the period of  
304 deposition, or that surface snow, through its roughness and porosity, acted as an accumulator of  
305 MPs through dry deposition shortly after the precipitation event. While the latter explanation is  
306 possible, the capture of only MP during the 12-h period following the precipitation event suggests  
307 that dry deposition was limited, possibly because snowfall acted to “clear” the atmosphere of  
308 suspended MPs.

309 There were no clear differences in the abundance or characteristics of MPs in snow samples  
310 between sites or between the different sample location types with two exceptions. Thus, firstly,  
311 the regular, black spherules observed at the sampling site close to a thermal power station suggests  
312 that combustion products were present that evaded destruction by peroxidation. Secondly, a greater  
313 fraction of grey-black fragments in the urban snows is consistent with greater capture or  
314 contamination by rubber tire-wear particles. The visual characteristics of these particles were often  
315 distinctly different from other MPs, being more elastic and less reflective.

316 SEM images indicated the presence of both “fresh”, unweathered MPs and “aged” and  
317 significantly degraded and contaminated MPs amongst the snow samples. This suggests that  
318 sources of MPs in the urban and remote settings may be both local and recent, and distal and older.  
319 For instance, the stress fractures evident in the sample illustrated in Figure 6a are similar to those

320 observed in MPs retrieved from the Lut and Kavir deserts (Abbasi et al., 2021), suggesting  
321 exposure to the harsh conditions of the arid regions to the south and southwest (Figure 2), while  
322 the tire-wear particles noted above appear to have more local origins in the urban setting. Such a  
323 variety of sources and histories, coupled with variations in terrain, population density, traffic  
324 intensity, turbulence and altitude between the sites, results in a heterogeneous assortment of MPs  
325 across the region sampled.

326 Overall, and within the constraints and operationalities of our methods, the mean and median  
327 concentrations of MP in snow samples were about 20 and 12 MP L<sup>-1</sup>, respectively, with no MPs  
328 evident in some samples and a maximum concentration of 86 MP L<sup>-1</sup>. These concentrations are  
329 substantially lower than the mean values reported by Bergmann et al. (2019) for fresh European  
330 snow and Arctic snow of unknown age (about 2500 and 1800 MP L<sup>-1</sup>, respectively). Here,  
331 however, particles were examined directly and without chemical separation by  $\mu$ -FTIR  
332 spectroscopy and the authors classified both synthetic and natural fibres and a variety of rubbers  
333 as plastic. Moreover, about 80% of the MPs detected by their  $\mu$ -FTIR were less than 25  $\mu$ m in size,  
334 which is below the detection limit of our microscopic approach (about 30  $\mu$ m).

335 More comparable with our study, Parolini et al. (2021) isolated MPs from subsurface snow in the  
336 Italian Alps by flotation in NaCl solution (density = 1.2 g cm<sup>-3</sup>) and identified particles  
337 microscopically. The authors report a mean concentration of 2.3 MP L<sup>-1</sup>, with fibres the most  
338 important type of MP but fragments and spherules also present. Pastorini et al. (2021) analysed  
339 three snow samples from the Italian Alps by  $\mu$ -FTIR after staining with Rose-Bengal and only  
340 detected one MP fibre in total (equivalent to 1 MP L<sup>-1</sup>). Napper et al. (2020) analysed fresh snow  
341 deposited on Mount Everest and found that concentrations identified by  $\mu$ -FTIR were in the range  
342 3 to 119 MP L<sup>-1</sup> (mean = 30 MP L<sup>-1</sup>). The majority of samples were fibrous and the most abundant

343 polymer was polyester, and while the authors suggested that tourists and climbers could make a  
344 significant, direct contribution to the pool of MPs, the sampling strategy adopted is more consistent  
345 with the collection of material deposited from the atmosphere.

346 An additional, useful comparison with the present results is with concentrations and characteristics  
347 of MPs in monthly precipitation (but mainly rainwater) sampled from a remote, elevated region of  
348 southern Iran (Mount Derak) and where plastics were defined, identified and quantified by  
349 precisely the same techniques (Abbasi and Turner, 2021). Here, and excluding one sample where  
350 the volume of precipitation was exceptionally small, concentrations ranged from 30 to 90 MP L<sup>-1</sup>  
351 (mean = 66 MP L<sup>-1</sup>; median = 60 MP L<sup>-1</sup>). Concentrations here reflect multiple events and may  
352 have been augmented by intermittent periods of dry deposition but the overall measures of central  
353 tendency are not that dissimilar to those observed in the snow samples from northern Iran. It is  
354 also worth noting that all MPs observed in precipitation samples from southern Iran were fibrous,  
355 that the dominant polymers were polypropylene, polystyrene and polyethylene, and that no  
356 samples were encountered in the largest size fraction ( $\geq 1000 \mu\text{m}$ ). In our snow samples, however,  
357 there was a greater diversity of shapes, sizes and polymer types (with different densities), with  
358 nylon and cellulose-based materials most abundant. These comparisons suggest that the amount  
359 of MPs deposited by rainfall and snow may be similar, but that the latter, perhaps because of the  
360 greater size, lower density and slower terminal velocity of snow particles relative to raindrops, is  
361 able to capture a greater variety and size distribution of MPs. Consistent with these observations,  
362 snow is known to be a better scavenger of coarse ( $> 4 \mu\text{m}$ ) aerosols than rainfall (Zhao et al., 2015).  
363 A greater scavenging capacity also renders snow as a more effective, as well as a simpler, synoptic  
364 indicator of atmospheric MP contamination than rainfall, and may reduce any confounding effects  
365 on precipitation fluxes associated with concurrent or intermittent dry deposition.

366 On melting of snow, MPs, along with other particulates and pollutants, will be carried into surface  
367 waters via runoff on impervious surfaces or into soil and groundwater and other vegetated surfaces  
368 (Zhu et al., 2012; Chen et al., 2018). However, it has also been suggested that MPs deposited with  
369 or after snowfall may accelerate the melting process itself (Ming and Wang, 2021). Here, coloured  
370 MPs, and in particular dark particles that have undergone weathering, may increase the absorption  
371 of solar radiation (or reduce the albedo) of fresh deposits of snow. More generally, this raises the  
372 possibility that MPs exert an impact on the Earth's radiative balance and climate.

373

## 374 **5. Conclusions**

375 This study has quantified and characterised MPs in fresh snow from a single precipitation event  
376 over a broad region of northern Iran. Concentrations of MPs were variable amongst samples and  
377 ranged from undetected to 86 MP per L of melted snow. There was no statistical difference in MP  
378 concentrations with depth of snow sampled or between urban and remote settings, with MPs  
379 reflecting a heterogeneous assortment of (mainly) fibres, fragments and films of different colours,  
380 sizes, polymer makeup and degrees of weathering. MPs appeared to be derived from both local  
381 and distal sources, with meteorological conditions and HYSPLIT modelling suggesting that MPs  
382 from the latter were brought into the area with northerly and southwesterly airflows. There appears  
383 to be a greater diversity of MPs in snow compared with rain sampled in southern Iran using the  
384 same protocols, and this may be attributed to the greater size and slower terminal velocities of  
385 snowflakes relative to raindrops. More studies are required to evaluate the mechanisms and global  
386 significance of snowfall in the capture and deposition of MPs from the atmosphere to soils and  
387 surface waters.

388

389 **Acknowledgements**

390 Funding for the study was provided by Shiraz University (Grant No. 99GRC1M371631).

391

392 **References**

393 Abbasi, S., Turner, A., 2021. Dry and wet deposition of microplastics in a semi-arid region  
394 (Shiraz, Iran). *Science of the Total Environment* 786, 147358.

395 Abbasi, S., Keshavarzi, B., Moore, F., Turner, A., Kelly, F.J., Dominguez, A.O., Jaafarzadeh, N.,  
396 2019. Distribution and potential health impacts of microplastics and microrubbers in air and  
397 street dusts from Asaluyeh County, Iran. *Environmental Pollution* 244, 153–164.

398 Abbasi, S., Turner, A., Hoseini, M., Amiri, H., 2021. Microplastics in the Lut and Kavir Deserts,  
399 Iran. *Environmental Science and Technology* 55, 5993-6000.

400 Allen, S., Allen, D., Phoenix, V.R., Le Roux, G., Jimenez, P.D., Simonneau, A., Binet, S.,  
401 Galop, D., 2019. Atmospheric transport and deposition of microplastics in a remote mountain  
402 catchment. *Nature Geoscience* 12, 339-344.

403 Allen, S., Allen, D., Moss, K., Le Roux, G., Phoenix, V.R., Sonke, J.E., 2020. Examination of  
404 the ocean as a source for atmospheric microplastics. *PLoS ONE* 15, e0232746.

405 Allen, S., Allen, D., Baladima, F., Phoenix, V. R., Thomas, J. L., Le Roux, G., Sonke, J. E.,  
406 2021. Evidence of free tropospheric and long-range transport of microplastic at Pic Du Midi  
407 Observatory. *Nature Communications* 12, 7242.

408 Bergmann, M.; Mützel, S.; Primpke, S.; Tekman, M.B.; Trachsel, J.; Gerdt, G. White and  
409 wonderful? Microplastics prevail in snow from the Alps to the Arctic. *Sci. Adv.* 2019, 5,  
410 eaax1157.

411 Brahney, J., Hallerud, M., Heim, E., Hahnenberger, M., Sukumaran, S., 2020. Plastic rain in  
412 protected areas of the United States. *Science* 368, 1257-1260.

413 Chen, L., Zhi, X., Shen, Z., Dai, Y., Aini, G., 2018. Comparison between snowmelt-runoff and  
414 rainfall-runoff nonpoint source pollution in a typical urban catchment in Beijing, China.  
415 *Environmental Science and Pollution Research* 25, 2377-2388.

416 Cowger W, Steinmetz Z, Gray A, Munno K, Lynch J, Hapich H, Primpke S, De Frond H,  
417 Rochman C, Herodotou O (2021). Microplastic Spectral Classification Needs an Open Source  
418 Community: Open Specy to the Rescue! *Analytical Chemistry*.  
419 <https://doi.org/10.1021/acs.analchem.1c00123>.

420 Dris, R., Gasperi, J., Mirande, C., Mandin, C., Guerrouache, M., Langlois, V., Tassin, B., 2017.  
421 A first overview of textile fibers, including microplastics, in indoor and outdoor environments.  
422 *Environ. Pollut.* 221, 453–458. <https://doi.org/10.1016/j.envpol.2016.12.013>.

423 Evangeliou, N., Grythe, H., Klimont, Z., Heyes, C., Eckhardt, S., Lopez-Aparicio, S., and Stohl,  
424 A., 2020. Atmospheric transport is a major pathway of microplastics to remote regions. *Nature*  
425 *Communications* 11, 1–11.

426 González-Pleiter, M., Edo, C., Aguilera, A., Viúdez-Moreiras, D., Pulido-Reyes, G., González-  
427 Toril, E., Osuna, S., de Diego-Castilla, G., Leganés, F., Fernández-Piñas, F., Rosal, R., 2021.  
428 Occurrence and transport of microplastics sampled within and above the planetary boundary  
429 layer. *Science of the Total Environment* 761, 143213.

430 Huang, Y.M., He, T., Yan, M.T., Yang, L., Gong, H., Wang, W.J., Qing, X., Wang, J., 2021.  
431 Atmospheric transport and deposition of microplastics in a subtropical urban environment.  
432 *Journal of Hazardous Materials* 416, 126168.

433 Huntington, A., Corcoran, P.L., Jantunen, L., Thaysen, C., Bernstein, S., Stern, G.A., Rochman,  
434 C.M., 2020. A first assessment of microplastics and other anthropogenic particles in Hudson Bay  
435 and the surrounding eastern Canadian Arctic waters of Nunavut. *Facets* 5, 432-454.

436 Klein, M., Fischer, E.K., 2019. Microplastic abundance in atmospheric deposition within the  
437 Metropolitan area of Hamburg, Germany. *Sci. Total Environ.* 685, 96–103.  
438 <https://doi.org/10.1016/j.scitotenv.2019.05.405>.

439 Liu, K., Wang, X., Song, Z., Wei, N., Haoda, Y., Cong, X., Zhao, L., Li, Y., Qu, L., Zhu, L.,  
440 Zhang, F., Zong, C., Jiang, C., Li, D., 2020. Global inventory of atmospheric fibrous  
441 microplastics input into the ocean: An implication from the indoor origin. *Journal of Hazardous*  
442 *Materials* 400, 123223.

443 Ming, J., Wang, F., 2021. Microplastics' hidden contribution to snow melting. *Eos Transactions*  
444 *American Geophysical Union* DOI: 10.1029/2021EO155631

445 Parolini, M.; Antonioli, D.; Borgogno, F.; Gibellino, M.C.; Fresta, J.; Albonico, C.; De Felice,  
446 B.; Canuto, S.; Concedi, D.; Romani, A.; Rosio, E., Gianotti, V., Laus, M., Ambrosini, R.,  
447 Cavallo, R., 2021. Microplastic contamination in snow from western Italian Alps. *Int. J. Environ.*  
448 *Res. Public Health* 18, 768. <https://doi.org/10.3390/ijerph18020768>

449 Pastorini, P., Pizzul, E., Bertoli, M., Anselmi, S., Kušće, M., Menconi, V., Prearo, M., Renzi, M.,  
450 2021. First insights into plastic and microplastic occurrence in biotic and abiotic compartments,  
451 and snow from a high-mountain lake (Carnic Alps). *Chemosphere* 265, 129121.

452 Parsa, V.A., Salehi, E., Yavari, A.R., van Bodegom, P.M., 2019. An improved method for  
453 assessing mismatches between supply and demand in urban regulating ecosystem services: A  
454 case study in Tabriz, Iran. *PLoS ONE* 14, e0220750.



455 Prata, J.C., da Costa, J.P., Girão, A.V., Lopes, I., Duarte, A.C., Rocha-Santos, T., 2019.  
456 Identifying a quick and efficient method of removing organic matter without damaging  
457 microplastic samples. *Science of the Total Environment* 686, 131-139.

458 Roblin, B., Ryan, M., Vreugdenhil, A., Aherne, J., 2020. Ambient atmospheric deposition of  
459 anthropogenic microfibers and microplastics on the western periphery of Europe (Ireland).  
460 *Environmental Science and Technology* 54, 11100-11108.

461 Skofronick-Jackson, G., Kulie, M., Milani, L., Munchak, S.J., Wood, N.B., Levizzani, V., 2019.  
462 Satellite estimation of falling snow: A global precipitation measurement (GPM) core observatory  
463 perspective. *Journal of Applied Meteorology and Climatology* 58, 1429-1448.

464 Wang, X.H., Liu, K., Zhu, L.X., Li, C.J., Song, Z.Y., Li, D.J., 2021. Efficient transport of  
465 atmospheric microplastics onto the continent via the East Asian summer monsoon. *Journal of*  
466 *Hazardous Materials* 414, 125477.

467 Zhang, Y., Kang, S., Allen, S., Allen, D., Gao, T., Sillanpää, M., 2020. Atmospheric  
468 microplastics: A review on current status and perspectives. *Earth-Science Reviews* 203, 103118.

469 Zhao, S., Yu, Y., He, J., Yin, D., Wang, B., 2015. Below-cloud scavenging of aerosol particles  
470 by precipitation in a typical valley city, northwestern China. *Atmos. Environ.* 102, 70–78.

471 Zhu, H., Xu, Y., Yan, B., Guan, J., 2012. Snowmelt runoff: A new focus of urban nonpoint  
472 source pollution. *International Journal of Environmental Research and Public Health* 9, 4333-  
473 4345.

474

475

476